

## Experimental Demonstration of Isotropic Negative Permeability in a Three-Dimensional Dielectric Composite

Qian Zhao,<sup>1,2</sup> Lei Kang,<sup>1</sup> B. Du,<sup>1</sup> H. Zhao,<sup>1</sup> Q. Xie,<sup>1</sup> X. Huang,<sup>1</sup> B. Li,<sup>1</sup> J. Zhou,<sup>1,\*</sup> and L. Li<sup>1</sup>

<sup>1</sup>State Key Lab of New Ceramics and Fine Processing, Department of Materials Science and Engineering, Tsinghua University, Beijing 100084, People's Republic of China

<sup>2</sup>State Key Lab of Tribology, Tsinghua University, Beijing 100084, People's Republic of China

(Received 20 June 2007; revised manuscript received 1 April 2008; published 11 July 2008)

Isotropic negative permeability resulting from Mie resonance is demonstrated in a three-dimensional (3D) dielectric composite consisting of an array of dielectric cubes. A strong subwavelength magnetic resonance, corresponding to the first Mie resonance, was excited in dielectric cubes by electromagnetic wave. Negative permeability is verified in the magnetic resonance area via microwave measurement and the dispersion properties. The resonance relies on the size and permittivity of the cubes. It is promising for construction of novel isotropic 3D left-handed materials with a simple structure.

DOI: 10.1103/PhysRevLett.101.027402

PACS numbers: 78.20.Ci, 41.20.Jb, 77.84.Lf, 77.90.+k

Negative refraction in left-handed metamaterials has attracted much attention on account of a range of unique properties [1–13]. Conventional approaches for obtaining negative refraction in the microwave to visible frequency range are based on complicated subwavelength metallic structures, such as metallic split ring resonators (SRRs) and wires [1–4],  $\Omega$ -shaped structures [5],  $U$ -shaped structures [6], staplelike structures [7], paired rods [8], and fishnet structures [9]. Such metallic structures exhibit electric or magnetic resonance at certain frequencies. The magnetic resonance in these metallic structures derives from the  $LC$  resonance, and depends on the dimensions and the dielectric environment of the structures [10,11]. However, due to the anisotropy of these metallic structures, negative refraction can only be performed in a certain direction [12]. Another drawback of the metal-based metamaterials is the difficulty in fabricating unit cells of complex geometry with submicron or nanoscale sizes for generation of negative permeability at infrared and optical frequencies [13]. As an alternative, the Mie resonance of dielectric particles provides a novel mechanism for the creation of magnetic and electric resonance, and offers a simpler and more versatile route for the production of isotropic metamaterials with higher frequencies.

The effective permeability and permittivity of an array of spherical particles embedded in a matrix was considered first by Levin [14]. For nonmagnetic spherical particles and matrix, the relative effective permeability of a dielectric composite, based on Levin's model, can be given by

$$\mu = 1 + \frac{3v}{\frac{F(\theta)+2}{F(\theta)-1} - v}, \quad (1)$$

where

$$F(\theta) = \frac{2(\sin\theta - \theta \cos\theta)}{(\theta^2 - 1)\sin\theta + \theta \cos\theta}. \quad (2)$$

In Eqs. (1) and (2), the volume fraction of the spherical

particles  $v = (4/3)\pi(r/a)^3$ ,  $\theta = k_0 r \sqrt{\epsilon_p}$ ,  $r$  and  $a$  are the particle radius and the lattice constant, and  $k_0$  and  $\epsilon_p$  are the free-space wave number and relative permittivity of particles, respectively.

Equation (2) shows that  $F(\theta)$  becomes infinite at certain frequencies, and therefore is negative for some values of  $\theta$ , resulting in a negative permeability as given by Eq. (1) [15]. By an appropriate choice of materials to satisfy the condition that the particles are small as compared to the wavelength in the matrix, negative permeability can be obtained. Recently, a few theoretical and simulated studies of negative refraction based on Mie resonance have been reported. These include metamaterials composed by arrays of magnetodielectric spheres [15], ferroelectric spheres [16], polaritonic spheres [13], and ferroelectric rods [17].

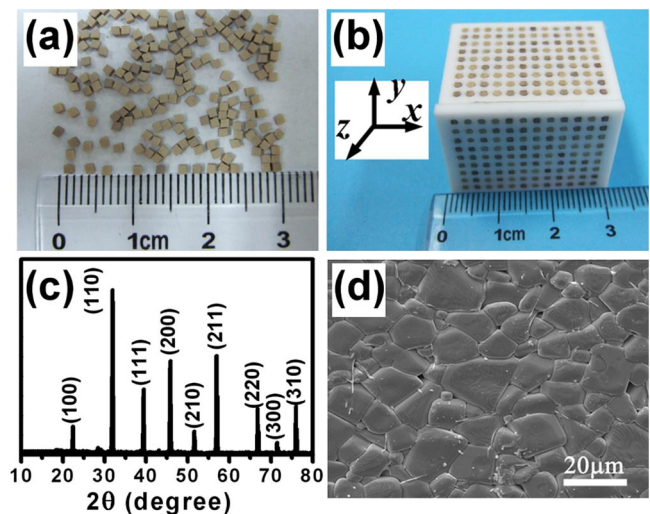


FIG. 1 (color online). The fabricated 3D dielectric composite. (a) Photograph of BST cubes with the side length of 1.0 mm. (b) Photograph of the simple cubic lattice of BST cubes arrayed in Teflon substrate. (c) XRD spectra of the BST cube. (d) SEM image.

Very recently, Peng *et al.* [18] reported an observation of left-handed behavior in a two-dimensional array of purely dielectric rods, where the second resonant mode was considered. This novel design opens the possibility of realizing media at terahertz frequencies. In this Letter, we focus on the feasibility of constructing an isotropic three-dimensional (3D) dielectric composite with negative permeability based on Mie resonance.

A dielectric ceramic material [ $\text{Ba}_{0.5}\text{Sr}_{0.5}\text{TiO}_3$  (BST)] was used to fabricate dielectric particles for its high permittivity and low loss at microwave frequencies. To simplify fabrication, cubes rather than spheres were used as the dielectric particles. Using a tape casting technique, BST green tapes with different thicknesses were fabricated and cut into cubes. The green cubes were then sintered at  $1450^\circ\text{C}$  for 6 h to attain compacted ceramic cubes [Fig. 1(a)]. The x-ray diffraction pattern [Fig. 1(c)] and scanning electron microscopy (SEM) image [Fig. 1(d)] reveal that the final cube samples are of phase  $\text{Ba}_{0.5}\text{Sr}_{0.5}\text{TiO}_3$  (JCPDS 39-1395) and are well crystallized. The density of the BST cubes is  $5.33\text{ g/cm}^3$ . The microwave permittivity of the BST cubes was measured using the Hakki-Coleman post resonator method, and determined as  $1600 + 4.8i$ . A simple cubic lattice of BST cubes was arrayed in a Teflon substrate with the permittivity of 2.1 [Fig. 1(b)]. The microwave transmission in the range 3–18 GHz was measured with an HP8720ES network analyzer using the rectangular waveguide method, which requires smaller sample size compared to the free-space method. Four different waveguides (WR-229, WR-137, WR-90, and WR-62) were used to ensure single-mode propagation in the measurements. Each sample is fabricated with different cross section and with the same length (3 cm) along the propagation direction to be placed in the waveguides. The microwaves propagate along the  $x$  axis, with the electric field polarized along the  $y$  axis and magnetic field polarized along the  $z$  axis.

To determine the magnetic resonance, the microwave transmissions of composites with different sizes of BST cubes were measured (shown as solid lines in Fig. 2). There are a series of resonance dips with different transmittance for each size of BST cube composite. The resonance dips lie at 6.12, 8.28, 11.40, and 12.92 GHz for the composite with a BST cube side length of  $l = 1.0$  mm and lattice constant of  $a = 2.5$  mm. These dips correspond to the multiple Mie resonance modes, and shift towards higher frequencies with decreasing cube side length, due to the blueshift of the Mie resonance as the particles become smaller. The first resonance dip is much sharper than the second one, implying a longer lifetime of the corresponding virtual bound state (Mie resonance) [19]. Additionally, theoretical transmission (dashed lines in Fig. 2) of BST cube array with two pairs of perfect electric walls and perfect magnetic walls bounding a propagation region was calculated using CST microwave studio. As can be seen, the measured resonance frequencies are in good agreement with those of the simulated results, especially

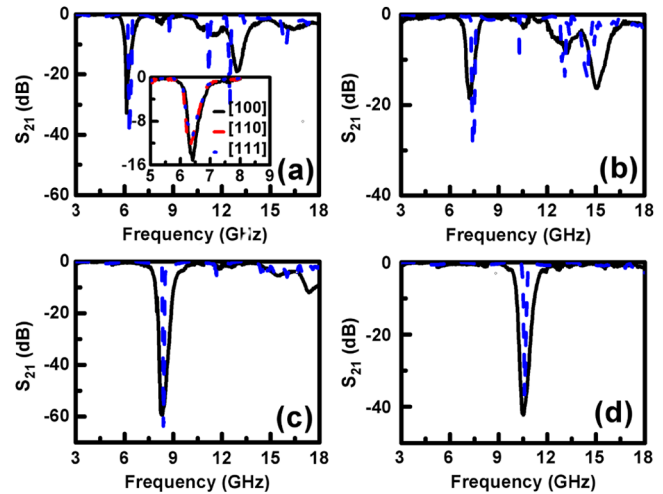


FIG. 2 (color online). Experimental (solid lines) and simulated (dashed lines) transmission for the dielectric composites with different side lengths of BST cube  $l$  and lattice constants  $a$ . (a)  $l = 1.0$  mm,  $a = 2.5$  mm. (b)  $l = 0.85$  mm,  $a = 1.6$  mm. (c)  $l = 0.75$  mm,  $a = 1.2$  mm. (d)  $l = 0.6$  mm,  $a = 1.1$  mm. Inset shows the transmissions along three different directions of [100], [110], and [111].

at the first Mie resonance. It is very time-consuming for the simulation performed in waveguide due to the large number of unit cells and high permittivity of BST cubes. And it is found that the microwaves with TE or TEM modes have little influence on the transmission of BST cube array. Therefore, the TEM mode is assumed in the simulation.

As expected from Mie resonance theory, each dielectric particle is equivalent to a magnetic dipole near the first resonant mode and to an electric dipole near the second one. To further determine the origin of the first and second resonance modes, the dynamic electric and magnetic field intensity distributions of a BST cube (Fig. 3) were calculated using CST Microwave Studio. It can be seen that the electric or magnetic fields are mainly localized in the cubes, and that the azimuthal component of the displacement current inside each cube is greatly enhanced at the first Mie resonance of 6.26 GHz [Fig. 3(a)], resulting in a large magnetic field along the  $z$  axis [Fig. 3(b)], corresponding to the  $\text{TE}_{011}$  mode of the Mie resonance. At the second Mie resonance of 8.62 GHz, the  $y$  component of the displacement current inside the cubes is greatly enhanced [Fig. 3(c)], resulting in a large magnetic field along the azimuth [Fig. 3(d)], which corresponds to the  $\text{TM}_{011}$  mode of the Mie resonance. The magnetic activity results from the enhancement of the displacement current inside each cube which, in turn, gives rise to a macroscopic bulk magnetization of the composite and a nonzero average magnetic susceptibility near the resonance [20]. It is known that resonant permeability or permittivity will generally lead to a generic dispersion curve. Therefore, we can determine whether the effective permeability is negative near the first resonance mode by analyzing the dispersion properties of the BST cubes.

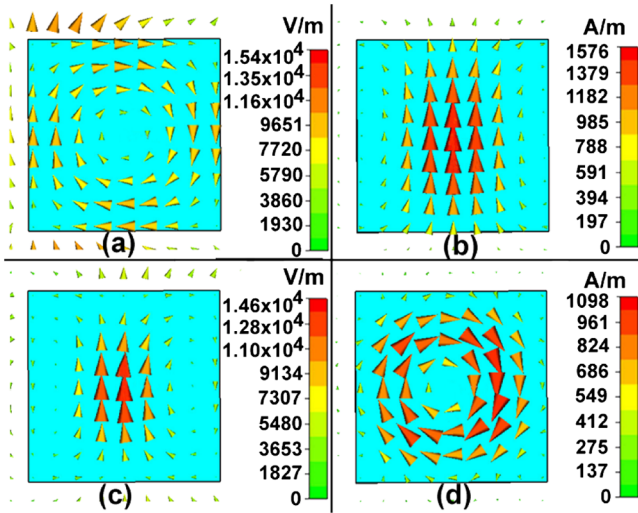


FIG. 3 (color online). Simulated dynamic electric and magnetic field intensity distribution in a BST cube with the magnetic and electric field polarized along the  $z$  and  $y$  axis. Electric field (a) in the plane  $z = 0$  and magnetic field (b) in the plane  $y = 0$  near the first Mie resonance. Electric field (c) in the plane  $z = 0$  and magnetic field (d) in the plane  $y = 0$  near the second Mie resonance.

Dispersion curves for the BST cubes filled in Teflon and for the combination of BST cubes and wires (diameter 0.3 mm) were calculated with the magnetic field polarized along the  $z$  axis and electric field polarized along the  $y$  axis (as shown in Fig. 4). For the BST cubes only [dashed line in Fig. 4(a)], there is a propagation forbidden band gap from 6.22 to 6.46 GHz. However, it is difficult to determine whether the gap is due to a resonance in the permeability or the permittivity. The periodically arrayed metallic wire medium, possessing a negative permeability below its plasma frequency, can be used to distinguish whether the band gap is attributed to negative permeability or permittivity [21]. If the band gap of the composite is due to negative permeability, the combination of the composite with a metallic wire medium should produce a resultant left-handed transmission. When wires are added symmetrically between the BST cubes, a passband (line with solid

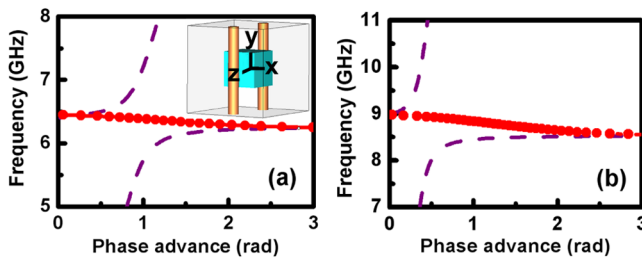


FIG. 4 (color online). Calculated dispersion curves for BST cubes only (dashed line), and for a combination of BST cubes and wires (line with solid circles). (a)  $l = 1.0$  mm,  $a = 2.5$  mm. (b)  $l = 0.75$  mm,  $a = 1.2$  mm. Inset shows the orientation of the BST cube and the wires.

circles) occurs within the previously forbidden band of the BST cube dispersion curves (dashed line), which indicates that the permeability is negative in the band gap. Two wires are used to increase the plasma frequency of the wire array and thus ensure that permittivity is negative within a broader frequency range. The imaginary part of the dispersion curve (not shown in Fig. 4) is very small in the left-handed band, which confirms the realization of a real passband of negative refractive index. The corresponding transmission experiments were also performed on the BST cube array with  $l = 0.75$  mm, wire array with the diameter of 0.3 mm and the combined BST cubes and metallic wires medium [Fig. 5(a)]. For the combined BST cubes and wires, a passband (solid line) is observed around the overlap of the forbidden bands of BST cubes array (dashed line) and the wire array (dotted line); i.e., negative permeability occurs in this region.

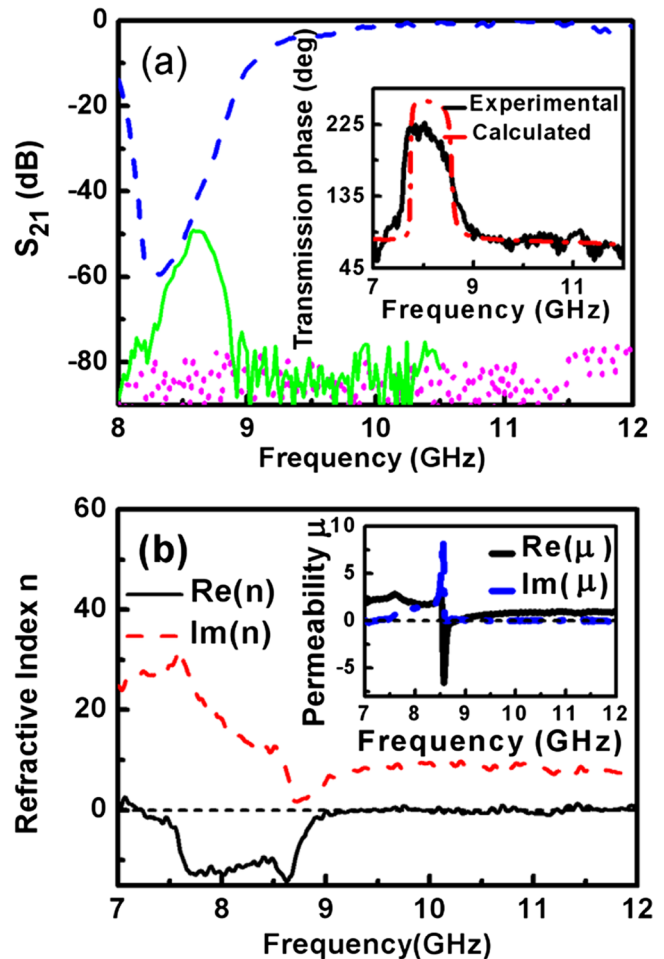


FIG. 5 (color online). (a) Transmission for the BST cube array with  $l = 0.75$  mm (dashed line), wire array only (dotted line), and the combination of BST cubes and wires (solid line). Inset of Fig. 5(a) shows the measured and calculated transmission phase of the sample with only one unit cell thickness along the propagation direction. (b) Retrieved refractive index and permeability (inset) based on the measured scattering parameters.



To retrieve the effective refractive index and permeability, the scattering parameters ( $S_{11}$  and  $S_{21}$ ) of the sample with only one unit cell along the propagation direction were experimentally measured. As shown in the inset of Fig. 5(a) that the measured transmission phase has a good agreement with the calculated one, and the reversed phase occurs in the range from 7.5 to 9.0 GHz, indicating a negative index band. The effective refractive index and permeability were retrieved using the methods [22] and shown in Fig. 5(b). It can be seen that the negative permeability is truly realized from 8.53 to 8.85 GHz in the fabricated dielectric composite. It is noted that the wider negative refraction range from 7.50 to 8.53 GHz is due to single negative effective parameters (negative permittivity and positive permeability), resulting from large imaginary part of index near the resonance as demonstrated in [23], rather than left-handed behavior.

This effective negative permeability only works, however, in the long-wavelength approximation. Figure 2 shows that the first Mie resonance is located at 6.12, 7.14, 8.30, and 10.50 GHz, for the cubes with  $l = 1.00$ , 0.85, 0.75, and 0.60 mm, respectively. For the composite with  $l = 1.0$  mm and  $a = 2.5$  mm, the wavelength of the magnetic resonance ( $\sim 49$  mm) exceeds the lattice constant by a factor of 20, which affirms the validity of the effective permeability in description of this composite. The measured transmissions along three different directions [inset of Fig. 2(a)], specifically [100], [110], and [111], show that the magnetic resonance is nearly independent of the transmission direction, and can thus be regarded as isotropic. If the BST cubes are replaced by spheres, it is expected that ideal isotropic negative permeability will be achieved.

Although the isotropic negative permeability is demonstrated in the 3D medium only at microwave frequencies, it is possible to extend this behavior down to shorter wavelengths because BST still has large permittivity of 200–300 in the terahertz range [24]. Additionally the magnetic activity based on Mie resonance can also be achieved within a broad frequency range from the terahertz to the deep infrared region by suitable choice of materials and particle dimensions, for example, polaritonic crystal ( $\text{LiTaO}_3$ ) have a permittivity of 400 at approximate 3.5 THz [17]. Moreover, the BST dielectric composites can be expected to possess electrically tunable properties, which may increase the range of potential applications [25,26].

In conclusion, we experimentally and numerically demonstrated isotropic negative effective permeability in a 3D dielectric composite. The negative effective permeability can be attributed to subwavelength magnetic resonance by the enhancement of the displacement current inside each dielectric cube, as distinct from the mechanism in metallic SRRs. The simple nonmetallic structure and isotropic 3D

left-handed behavior of such dielectric composites make them a promising candidate for designing cloaking devices [27].

This work is supported by the National Science Foundation of China under Grants No. 50425204, No. 50621201, No. 50632030, No. 50721004, and No. 10774087, and by the Postdoctoral Science Foundation under Grants No. 20060390043 and No. 20060400054. The authors gratefully acknowledge discussions with Professor J.A. Kong, Professor A. Godfrey, Dr. F.L. Zhang, C.H. Liang, Z.W. Yang, R. Wang, and F. Zhao.

---

\*Author to whom correspondence should be addressed.  
zhouji@mail.tsinghua.edu.cn

- [1] J. B. Pendry, *Phys. Rev. Lett.* **85**, 3966 (2000).
- [2] R. Shelby, D. R. Smith, and S. Schultz, *Science* **292**, 77 (2001).
- [3] A. A. Houck, J. B. Brock, and I. L. Chuang, *Phys. Rev. Lett.* **90**, 137401 (2003).
- [4] C. G. Parazzoli *et al.*, *Phys. Rev. Lett.* **90**, 107401 (2003).
- [5] J. Huangfu *et al.*, *Appl. Phys. Lett.* **84**, 1537 (2004).
- [6] C. Enkrich *et al.*, *Phys. Rev. Lett.* **95**, 203901 (2005).
- [7] S. Zhang *et al.*, *Phys. Rev. Lett.* **94**, 037402 (2005).
- [8] V. M. Shalaev *et al.*, *Opt. Lett.* **30**, 3356 (2005).
- [9] G. Dolling *et al.*, *Opt. Lett.* **31**, 1800 (2006).
- [10] J. B. Pendry *et al.*, *IEEE Trans. Microwave Theory Tech.* **47**, 2075 (1999).
- [11] Q. Zhao *et al.*, *Appl. Phys. Lett.* **90**, 011112 (2007).
- [12] P. Gay-Balmaz and O. J. F. Martin, *Appl. Phys. Lett.* **81**, 939 (2002).
- [13] M. S. Wheeler, J. S. Aitchison, and M. Mojahedi, *Phys. Rev. B* **72**, 193103 (2005).
- [14] L. Lewin, *Proc. Inst. Electr. Eng.* **94**, 65 (1947).
- [15] C. L. Holloway *et al.*, *IEEE Trans. Antennas Propag.* **51**, 2596 (2003).
- [16] O. G. Vendik and M. S. Gashinova, *Proceedings of the 34th European Microwave Conference, Amsterdam* (IEEE Press, Piscataway, NJ, 2004), Vol. 3, p. 1209.
- [17] K. C. Huang, M. L. Povinelli, and J. D. Joannopoulos, *Appl. Phys. Lett.* **85**, 543 (2004).
- [18] L. Peng *et al.*, *Phys. Rev. Lett.* **98**, 157403 (2007).
- [19] V. Yannopoulos and A. Moroz, *J. Phys. Condens. Matter* **17**, 3717 (2005).
- [20] S. O'Brien and J. B. Pendry, *J. Phys. Condens. Matter* **14**, 4035 (2002).
- [21] D. R. Smith *et al.*, *Phys. Rev. Lett.* **84**, 4184 (2000).
- [22] X. Chen *et al.*, *Phys. Rev. E* **70**, 016608 (2004).
- [23] S. Zhang *et al.*, *Phys. Rev. Lett.* **95**, 137404 (2005).
- [24] G. Vélú *et al.*, *Ferroelectrics* **353**, 29 (2007).
- [25] B. Hou *et al.*, *Opt. Express* **13**, 9149 (2005).
- [26] Q. Zhao *et al.*, *Appl. Phys. Lett.* **89**, 221918 (2006).
- [27] D. P. Gaillot, C. Croënne, and D. Lippens, *Opt. Express* **16**, 3986 (2008).